Centrum voor Wiskunde en Informatica

REPORTRAPPORT

MAS

Modelling, Analysis and Simulation

MAS

Modelling, Analysis and Simulation

Computing the real parabolic cylinder functions *U(a,x)*, *V(a,x)*

A. Gil, J. Segura, N.M. Temme

REPORT MAS-E0612 APRIL 2006

Centrum voor Wiskunde en Informatica (CWI) is the national research institute for Mathematics and Computer Science. It is sponsored by the Netherlands Organisation for Scientific Research (NWO).
CWI is a founding member of ERCIM, the European Research Consortium for Informatics and Mathematics.

CWI's research has a theme-oriented structure and is grouped into four clusters. Listed below are the names of the clusters and in parentheses their acronyms.

Probability, Networks and Algorithms (PNA)

Software Engineering (SEN)

Modelling, Analysis and Simulation (MAS)

Information Systems (INS)

P.O. Box 94079, 1090 GB Amsterdam (NL)
Kruislaan 413, 1098 SJ Amsterdam (NL)
Telephone +31 20 592 9333
Telefax +31 20 592 4199

ISSN 1386-3703

Computing the real parabolic cylinder functions *U(a,x), V(a,x)*

ABSTRACT

Methods for the computation of real parabolic cylinder functions *U(a,x)* and *V(a,x)* and their derivatives are described. We give details on power series, asymptotic series, recursion and quadrature. A combination of these methods can be used for computing parabolic cylinder functions for unrestricted values of the order *a* and the variable *x* except for the overflow/underflow limitations. By factoring the dominant exponential factor, scaled functions can be computed without practical overflow/underflow limitations. In an accompanying paper we describe the precise domains for these methods and we present the Fortran 90 codes for the computation of these functions.

2000 Mathematics Subject Classification: 33C15, 41A60, 65D20, 65D32
1998 ACM Computing Classification System: G4
Keywords and Phrases: parabolic cylinder functions, non-oscillating integral representations, numerical quadrature, asymptotic expansions
Note: This report is accepted for publication in ACM-TOMS.

Computing The Real Parabolic Cylinder Functions $U(a, x)$, $V(a, x)$

Amparo Gil
Departamento de Matemáticas, Estadística y Computación, U. de Cantabria, 39005-Santander, Spain

Javier Segura
Departamento de Matemáticas, Estadística y Computación, U. de Cantabria, 39005-Santander, Spain

and
Nico M. Temme
CWI, P.O. Box 94079, 1090 GB Amsterdam, The Netherlands

Methods for the computation of real parabolic cylinder functions $U(a, x)$ and $V(a, x)$ and their derivatives are described. We give details on power series, asymptotic series, recursion and quadrature. A combination of these methods can be used for computing parabolic cylinder functions for unrestricted values of the order a and the variable x except for the overflow/underflow limitations. By factoring the dominant exponential factor, scaled functions can be computed without practical overflow/underflow limitations. In an accompanying paper we describe the precise domains for these methods and we present the Fortran 90 codes for the computation of these functions.

Categories and Subject Descriptors: G.4 [**Mathematics of Computing**]: Mathematical software

General Terms: Algorithms

Additional Key Words and Phrases: Parabolic cylinder functions, non-oscillating integral representations, numerical quadrature, asymptotic expansions.

1. INTRODUCTION

In this paper, we describe methods for the computation of the parabolic cylinder functions (PCFs) $U(a, x)$, $V(a, x)$, and their derivatives, for real values of a and x. Although parabolic cylinder functions appear in a vast number of applications in mathematics, physics and engineering (see for instance [11]), there are no available numerical algorithms with a verified accuracy for the evaluation of PCFs for real a and x. This article and the accompanying paper and routines are intended to fill this gap.

For an overview of properties of these functions we refer to [1, Chapter 19]. The functions $U(a, x)$, $V(a, x)$ are the two standard linearly independent solutions of the differential equation:

$$\frac{d^2w}{dx^2} - \left(\tfrac{1}{4}x^2 + a\right) w = 0\,, \tag{1}$$

with initial conditions

$$\begin{aligned} U(a,0) &= \frac{\sqrt{\pi}}{2^{a/2+1/4}\Gamma(\frac{3}{4}+\frac{1}{2}a)}\,, \qquad U'(a,0) = -\frac{\sqrt{\pi}}{2^{a/2-1/4}\Gamma(\frac{1}{4}+\frac{1}{2}a)}\,, \\ V(a,0) &= \frac{2^{a/2+1/4}\sin\pi(\frac{3}{4}-\frac{1}{2}a)}{\Gamma(\frac{3}{4}-\frac{1}{2}a)}\,,\ V'(a,0) = \frac{2^{a/2+3/4}\sin\pi(\frac{1}{4}-\frac{1}{2}a)}{\Gamma(\frac{1}{4}-\frac{1}{2}a)}\,. \end{aligned} \tag{2}$$

The Wronskian relation for $U(a,x)$ and $V(a,x)$ reads

$$\mathcal{W}[U(a,x),V(a,x)] = \sqrt{\frac{2}{\pi}}. \tag{3}$$

They constitute a numerically satisfactory pair for $x > 0$, in the sense described by Miller [8] because

$$U(a,x) \sim x^{-a-1/2}e^{-x^2/4}(1+\mathcal{O}(x^{-2}))\,, \quad V(a,x) \sim \sqrt{\frac{2}{\pi}}x^{a-1/2}e^{x^2/4}(1+\mathcal{O}(x^{-2}))\,, \tag{4}$$

as $x \to \infty$.

Because equation (1) is invariant under the change of variable $x \to -x$ both $U(a,-x)$ and $V(a,-x)$ are also solutions of (1). Given that $\{U(a,x), V(a,x)\}$ constitute a numerically satisfactory pair of independent solutions for $x \geq 0$, we can compute $U(a,x)$ and $V(a,x)$ for $x < 0$ by writing them as linear combinations of $U(a,-x)$ and $V(a,-x)$, $x < 0$.

The following relations can be applied if the values of $U(a,x)$ and $V(a,x)$ are required for $x < 0$:

$$\begin{aligned} U(a,x) &= \Gamma(\tfrac{1}{2}-a)\cos(\pi a)V(a,-x) - \sin(\pi a)U(a,-x)\,, \\ V(a,x) &= \sin(\pi a)V(a,-x) + \frac{\cos(\pi a)}{\Gamma(\frac{1}{2}-a)}U(a,-x)\,, \end{aligned} \tag{5}$$

for $a \leq 0$, and

$$\begin{aligned} U(a,x) &= \frac{\pi}{\Gamma(\frac{1}{2}+a)}V(a,-x) - \sin(\pi a)U(a,-x)\,, \\ V(a,x) &= \sin(\pi a)V(a,-x) + \frac{\cos^2(\pi a)}{\pi}\Gamma(\tfrac{1}{2}+a)U(a,-x)\,, \end{aligned} \tag{6}$$

when $a \geq 0$.
Notice, however, that $U(a,x)$ and $V(a,x)$ do not constitute a numerically satisfactory pair for $x < 0$ except when $a = -(2k-1)/2$, $k \in \mathbb{N}$ or $a = k$, $k \in \mathbb{Z}$.

In the sequel we restrict the discussion to $x \geq 0$.

2. DEFINITION OF SCALED FUNCTIONS

For large values of the parameters a and x the PCFs become very large or very small. To avoid overflow or underflow in numerical computations [7] and to improve the condition of the function evaluation (see Section 10) it is important to define scaled values with the dominant exponential behavior factored out. Appropriate scaling factors can be deduced from the integral representations in Section 9 (see also [6]), the scaling factor being related to the contribution at the saddle point; this scaling factor can be also factored out from the uniform asymptotic expansions of Section 6 (see also [12]).

The following quantity

$$f(a,x) = \left(\frac{x}{2} + \sqrt{\frac{x^2}{4} + a}\right)^a \exp\left(\frac{x}{2}\sqrt{\frac{x^2}{4} + a} - \frac{a}{2}\right) \tag{7}$$

plays a role as a dominant exponential factor. This function is real in the monotonic region $x^2/4 + a \geq 0$ and gets an imaginary part in the oscillatory region.

As a function of

$$t = \frac{x}{2\sqrt{|a|}} \tag{8}$$

$f(a,x)$ can be written as

$$f(a,x) = f(a)e^{2|a|\Theta}\,, \tag{9}$$

where (using the same notation as in [12] and [6])

$$\Theta = \begin{cases} \tilde{\xi} \equiv \frac{1}{2}\left[t\sqrt{t^2+1} + \log(t + \sqrt{t^2+1})\right] & ,\ a > 0 \\ \xi \equiv \frac{1}{2}\left[t\sqrt{t^2-1} - \log(t + \sqrt{t^2-1})\right] & ,\ a < 0, t > 1 \\ i\eta = \frac{i}{2}\left[\arccos t - t\sqrt{1-t^2}\right] & ,\ a < 0, 0 \leq t \leq 1 \end{cases} \tag{10}$$

In the oscillatory region $x^2/4 + a < 0$ (that is, $a < 0$ and $0 \leq t < 1$), the values for the square roots in Eq. (7) are taken in the principal branch. In this region, the imaginary part indicates that the parabolic cylinder functions oscillate with a phase function $\phi(a,x) \sim 2a\eta$ as $a \to -\infty$, as we will later see explicitly in the expressions of the asymptotic expansions and integral representations in this region.

Because we are dealing with real parabolic cylinder functions, we will not include in our scaling factor the exponential of imaginary argument. Instead, we define the scaling factor as:

$$F(a,x) = |f(a,x)|\,. \tag{11}$$

For the oscillatory domain the scaling factor will be also denoted by

$$f(a) \equiv |f(a,x)| = |a|^{a/2}e^{-a/2}. \tag{12}$$

The scaled PCFs for $x \geq 0$ are defined as follows

$$\begin{array}{ll} \widetilde{U}(a,x) = F(a,x)U(a,x)\,, & \widetilde{U'}(a,x) = F(a,x)U'(a,x)\,, \\ \widetilde{V}(a,x) = \dfrac{V(a,x)}{F(a,x)}\,, & \widetilde{V'}(a,x) = \dfrac{V'(a,x)}{F(a,x)}\,. \end{array} \tag{13}$$

3. METHODS OF COMPUTATION

Different strategies of computation should be considered depending on the range of the variable and the order a. Namely:

(1) Maclaurin series for small x.

(2) Poincaré asymptotic expansions for large x and moderate a .

(3) Uniform asymptotic expansions in terms of elementary functions for large $|a|$:
   (a) Expansions in the monotonic region $x^2 > -4a$
   (b) Expansions in the oscillatory region $x^2 < -4a$

(4) Uniform Airy-type asymptotic expansions around the turning points $x^2 = -4a$ and large $-a$

(5) Integral representations when the previous methods fail
   (a) In the monotonic region $x^2 > -4a$ both for $a > 0$ and $a < 0$
   (b) In the oscillatory region $x^2 < -4a$

(6) Recurrence relations when other methods become inefficient or when they fail.

In [7] we describe in detail the different regions where each method is preferable for speed and accuracy considerations.

Figure 1 shows a sketch of the use of the different methods in the (x, a)-plane for moderate values of a and x. In particular, the figure shows the selection of methods considered in the codes described in [7] (relative precision $5\,10^{-14}$). The computations for $U(a, x)$ and $U'(a, x)$ are based on the same method in each region in the (a, x)-plane and the same is true for $V(a, x)$ and $V'(a, x)$.

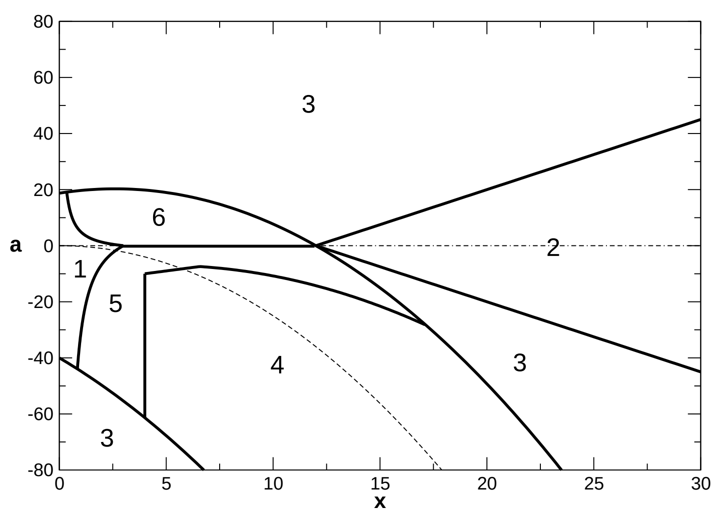

Figure 1. Regions where the different methods of computation are used. **1**: Maclaurin series; **2**: Poincaré asymptotic expansions; **3**: uniform asymptotic expansions in terms of elementary

functions; **4**: uniform Airy-type asymptotic expansions; **5**: integral representations; **6**: recurrences for $U(a,x)$ (with starting values above region 6) and Maclaurin series for $V(a,x)$.

These regions of computation can be chosen differently because the methods have regions of overlapping validity; in this case, the fastest methods should be considered. In particular, the integral representations we will develop cover the whole plane with few exceptions ($|a|$ small; $|x|$ small and a positive semi-integer). Therefore, quadrature can be used as a validation of other methods and it is a *guard method* which can be used when all other methods become insufficient or fail.

In the following sections we describe these different methods of computation.

4. MACLAURIN SERIES

Maclaurin series are used for small x both for $U(a,x)$, $V(a,x)$. These series are given in [1] pp. 686-687.

The even and odd series solutions of Eq. (1) are given by (19.2.5) and (19.2.6) of [1]:

$$\begin{aligned} y_1(a,x) &= \left\{1 + a\frac{x^2}{2!} + (a^2+1/2)\frac{x^4}{4!} + ...\right\}, \\ y_2(a,x) &= \left\{x + a\frac{x^3}{3!} + (a^2+3/2)\frac{x^5}{5!} + ...\right\}. \end{aligned} \tag{14}$$

The coefficients in front of $x^k/k!$ in (14), which we denote by a_k, satisfy the following recurrence relation

$$a_{n+2} = a a_n + \tfrac{1}{4}n(n-1)a_{n-2}, \quad n = 2,3,4,\ldots, \tag{15}$$

with $a_0 = a_1 = 1$.

In terms of the even and odd solutions, the functions $U(a,x)$ and $V(a,x)$ can be written as:

$$\begin{aligned} U(a,x) &= U(a,0)y_1(a,x) + U'(a,0)y_2(a,x), \\ V(a,x) &= V(a,0)y_1(a,x) + V'(a,0)y_2(a,x), \end{aligned} \tag{16}$$

the initial conditions being given by Eq. (2). The derivatives are easily obtained from Eq. (14).

When considering a stopping criterion for the evaluation of the series in Eq. (14) it is important to take into account that the coefficients accompanying the even (odd) powers of x in the $y_1(a,x)$ ($y_2(a,x)$) series become zero at $a = 0$. A common stopping criterion consists in adding terms until the last term adds a contribution to the total sum smaller than the demanded relative accuracy. In this case, this criterion is dangerous because some terms become zero as $a \to 0$. A way to circumvent this problem is by adding two terms in each iteration. It is also worth noticing that the representation considered here ([1], formulas 19.2.5-19.2.7) is preferable over the representation in terms of confluent hypergeometric functions ([1], formulas 19.2.1-19.2.4). Indeed, the latter unavoidably suffers from cancellation problems as $a \to 0$.

Usually, scaled functions will not be needed in the region **1** of Figure 1 because the values of $|a|$ and x do not become very large and, for moderate values of a and x, scaled functions can be safely obtained by multiplying or dividing the functions by $F(a,x)$ (Eq. (13)). However, Maclaurin series are a useful method of computation of the V-function for large positive a and x very close to 0 due to the cancellation of $V(a,0)$ and $V'(a,0)$ for some values of a.

For positive a the initial conditions for the V-function can be written as

$$\begin{aligned} V(a,0) &= \frac{2^{a/2-3/4}}{\pi}(1+\sin\pi a)\Gamma(\tfrac14+\tfrac{a}{2})\,, \\ V'(a,0) &= \frac{2^{a/2-1/4}}{\pi}(1-\sin\pi a)\Gamma(\tfrac34+\tfrac{a}{2})\,, \end{aligned} \tag{17}$$

and therefore $V(2k-\frac32,0)=0,\ k\in\mathbb{N}$ and $V'(2k-\frac12,0)=0,\ k\in\mathbb{N}$. This corresponds to the case of Hermite polynomials. Of course, close to the points $(2k-1/2,0)$ and $(2k-3/2,0)$ we can expect loss of relative precision. This loss of precision is better under control with Maclaurin series than with the rest of available methods (integrals and uniform asymptotics). Indeed, these cancellations are exact up to the usual rounding error limitations because they are caused by the factors $1\pm\sin\pi a$ in Eq. (17); contrary, the cancellation in Eqs. (34) and (107) is approximate. For this reason, it is convenient to use Maclaurin series also for large $a>0$ and small x.

For computing series for large $a>0$, it is necessary to scale the starting values in order to avoid overflow/underflow problems. Namely, we have:

$$\begin{aligned} \widetilde{U}(a,x) &= u_1 y_1(a,x) + u_2 y_2(a,x)\,, \\ \widetilde{V}(a,x) &= v_1 y_1(a,x) + v_2 y_2(a,x)\,, \end{aligned} \tag{18}$$

and the coefficients are

$$\begin{aligned} u_1 &\equiv F(a,x)U(a,0) = \frac{1}{\sqrt{2}}H(a)e^{2a\tilde{\xi}}\,, \\ u_2 &\equiv F(a,x)U'(a,0) = -\frac{\beta(a)}{\sqrt{2}H(a)}e^{2a\tilde{\xi}}\,, \\ v_1 &\equiv \frac{1}{F(a,x)}V(a,0) = \frac{1+\sin\pi a}{\sqrt{\pi}}\frac{H(a)}{\beta(a)}e^{-2a\tilde{\xi}}\,, \\ v_2 &\equiv \frac{1}{F(a,x)}V'(a,0) = \frac{1-\sin\pi a}{\sqrt{\pi}}\frac{1}{H(a)}e^{-2a\tilde{\xi}}\,, \end{aligned} \tag{19}$$

where $\tilde{\xi}$ is defined in Eq. (10),

$$H(a) = \frac{\beta\left(\dfrac14+\dfrac{a}{2}\right)}{\left(a+\dfrac12\right)^{1/4}\left[S\left(\dfrac{1}{2a}\right)\right]^{1/4}}\,, \tag{20}$$

$$\beta(\lambda) = \frac{\sqrt{2\pi}\lambda^{\lambda}e^{-\lambda}}{\Gamma\left(\lambda+\dfrac12\right)} \sim 1 \text{ as } \lambda\to+\infty \tag{21}$$

and

$$S(y) = \frac{1}{e}(1+y)^{1/y} \sim 1 \text{ as } y \to 0. \tag{22}$$

For large a and in order to avoid overflows, asymptotic expansions for $\beta(\frac{1}{4}+\frac{a}{2})$ and $S((2a)^{-1})$ are a convenient way of computing these functions. Later, we give details for the computation of β.

5. POINCARÉ EXPANSIONS FOR X LARGE

The asymptotic formulas for $x >> |a|$ for the U and V functions are given by Eqs. 19.8.1 and 19.8.2 of [1]. Asymptotic expansions for the derivative can be obtained by differentiating both formulas. We have

$$\begin{aligned} U(a,x) &\sim \frac{1}{\sqrt{x}\psi(a,x)}\sum_{k=0}^{\infty}\frac{a_k}{x^{2k}}\,, \quad U'(a,x) \sim -\frac{\sqrt{x}}{2\psi(a,x)}\sum_{k=0}^{\infty}\frac{b_k}{x^{2k}}\,, \\ V(a,x) &\sim \sqrt{\frac{2}{\pi x}}\psi(a,x)\sum_{k=0}^{\infty}\frac{c_k}{x^{2k}}\,,\ V'(a,x) \sim \sqrt{\frac{x}{2\pi}}\psi(a,x)\sum_{k=0}^{\infty}\frac{d_k}{x^{2k}}\,, \end{aligned} \tag{23}$$

where

$$\psi(a,x) = x^a e^{x^2/4} \tag{24}$$

and the coefficients can be computed recursively in the following way:

$$\begin{aligned} a_k &= -\frac{(a+2k-3/2)(a+2k-\frac{1}{2})}{2k}a_{k-1}\ ; \quad && a_0 = 1\,, \\ b_k &= a_k + (2a+4k-3)a_{k-1}\ ; && b_0 = 1\,, \\ c_k &= \frac{(a-2k+3/2)(a-2k+\frac{1}{2})}{2k}c_{k-1}\ ; && c_0 = 1\,, \\ d_k &= c_k + (2a-4k+3)c_{k-1}\ ; && d_0 = 1\,. \end{aligned} \tag{25}$$

Regarding the evaluation of scaled functions care must be taken because, as $x \to \infty$, $\psi(a,x)/F(a,x) \to 1$ and then a straightforward computation of this ratio may cause cancellations. The scaled asymptotic expansions read

$$\begin{aligned} \widetilde{U}(a,x) &\sim \frac{1}{\sqrt{x}\phi(a,x)}\sum_{k=0}^{\infty}\frac{a_k}{x^{2k}}\,, \quad \widetilde{U'}(a,x) \sim -\frac{\sqrt{x}}{2\phi(a,x)}\sum_{k=0}^{\infty}\frac{b_k}{x^{2k}}\,, \\ \widetilde{V}(a,x) &\sim \sqrt{\frac{2}{\pi x}}\phi(a,x)\sum_{k=0}^{\infty}\frac{c_k}{x^{2k}}\,,\ \widetilde{V'}(a,x) \sim \sqrt{\frac{x}{2\pi}}\phi(a,x)\sum_{k=0}^{\infty}\frac{d_k}{x^{2k}}\,, \end{aligned} \tag{26}$$

where $\phi(a,x) = \psi(a,x)/F(a,x)$ can be written as

$$\phi(a,x) = \left(\frac{2}{1+\sqrt{1+4a/x^2}}\right)^a \exp\left(2\left(\frac{a}{x(1+\sqrt{1+4a/x^2})}\right)^2\right)\,. \tag{27}$$

6. UNIFORM ASYMPTOTIC EXPANSIONS IN TERMS OF ELEMENTARY FUNCTIONS

We also consider asymptotic expansions for $U(a,x)$ and $V(a,x)$ in terms of elementary functions. Additional details on these expansions can be found in [12].

6.1 Expansions for $x \ge 0$, $|a| + x >> 0$, $\frac{x^2}{4} + a > 0$ (monotonic region)

In the non-oscillating region, it is possible to derive unified expressions (for $a > 0$ and $a < 0$) from those given in [12] by restoring in these expressions the original variables. The expansions are valid for $|a| \to \infty$ uniformly with respect to $x \ge 0$ (when $a \to +\infty$) and with respect to $t = x/(2\sqrt{|a|}) \in [1+\epsilon, \infty)$ (when $a \to -\infty$), where ϵ is a small positive number. These expansions have the double asymptotic property of being valid for fixed t and large $|a|$ and for fixed a and large t.

The scaled U functions can be obtained from Eqs. (2.29) and (2.33) of [12] for $a \ge 0$ and (2.9) and (2.18) of [12] for $a \le 0$. The expansions for $a \ge 0$ and $a \le 0$ are in fact the same and they follow from the representations:

$$\begin{aligned} \widetilde{U}(a,x) &= \frac{1}{\sqrt{2}}\left(\frac{x^2}{4}+a\right)^{-1/4} F_a\,, \\ \widetilde{U'}(a,x) &= -\frac{1}{\sqrt{2}}\left(\frac{x^2}{4}+a\right)^{1/4} G_a\,, \end{aligned} \tag{28}$$

where F_a and G_a have the expansions

$$F_a \sim \sum_{s=0}^{\infty} \frac{\phi_s(\tau)}{(-2a)^s}\ ;\ G_a \sim \sum_{s=0}^{\infty} \frac{\psi_s(\tau)}{(-2a)^s}\ ; \tag{29}$$

$$\tau = \frac{1}{2}\left[\frac{x/2}{\sqrt{x^2/4+a}} - 1\right] = \frac{-a/2}{x^2/4 + a + \frac{x}{2}\sqrt{x^2/4+a}}\,. \tag{30}$$

The coefficients $\phi_s(\tau)$ are polynomials in τ which follow from the recursion ([12], Eq. (2.11))

$$\phi_{s+1}(\tau) = -4\tau^2(\tau+1)^2\frac{d\phi_s(\tau)}{d\tau} - \frac{1}{4}\int_0^{\tau}(20\tau'^2+20\tau'+3)\phi_s(\tau')d\tau'\,, \tag{31}$$

with $\phi_0(\tau) = 1$, $\phi_{-1}(\tau) = 0$.

The coefficients $\psi_s(\tau)$ can be obtained from the relation ([12], Eq. (2.16))

$$\psi_s(\tau) = \phi_s(\tau) + 2\tau(\tau+1)(2\tau+1)\phi_{s-1}(\tau) + 8\tau^2(\tau+1)^2\frac{d\phi_{s-1}(\tau)}{d\tau}\,. \tag{32}$$

Asymptotic expansions for the $V-$function and its derivative (or the corresponding scaled functions) can be obtained from the expansions for $U(a,x)$ and its derivative, together with the analogous expansions for $U(a,-x)$, $x \ge 0$, and the formula

$$V(a,x) = \frac{\Gamma(a+\frac{1}{2})}{\pi}\left[\sin\pi a\, U(a,x) + U(a,-x)\right]\,. \tag{33}$$

In this way, combining the expansions of Eq. (28) and the expansions for $U(a,-x)$, $x \geq 0$, $a \geq 0$, $a - x >> 0$ ([12], Eq. (2.34)) we obtain the following representations for the scaled $V-$functions when $a > 0$:

$$\begin{aligned} \widetilde{V}(a,x) &= \frac{1}{\sqrt{\pi}}\left(\frac{x^2}{4}+a\right)^{-1/4}\left[P_a + \sin\pi a M(a,x) F_a\right] , \\ \widetilde{V}'(a,x) &= \frac{1}{\sqrt{\pi}}\left(\frac{x^2}{4}+a\right)^{1/4}\left[Q_a - \sin\pi a M(a,x) G_a\right] , \end{aligned} \tag{34}$$

where

$$M(a,x) = \frac{\Gamma(a+\frac{1}{2})}{\sqrt{2\pi}F(a,x)^2} \tag{35}$$

and P_a and Q_a have the expansions

$$P_a \sim \sum_{s=0}^{\infty}\frac{\phi_s(\tau)}{(2a)^s}\ ;\ Q_a \sim \sum_{s=0}^{\infty}\frac{\psi_s(\tau)}{(2a)^s}\ , \tag{36}$$

with $F(a,x)$ as given in Eq. (11). For large a the ratio $M(a,x)$ should be computed with care because both the numerator and the denominator tend to overflow. The factor $M(a,x)$ can be written as

$$M(a,x) = e^{-4a\widetilde{\xi}}\beta(a)^{-1}, \tag{37}$$

where $\widetilde{\xi}$ is given by Eq. (10) and $\beta(a)$ is given by Eq. (21); $\beta(a)$ can be computed by means of an asymptotic expansion when a is large. We give more details on this expansion in the next section.

The seconds terms in Eq. (34) should be dropped when the factor $M(a,x)$ tends to underflow. For fixed a the factor $M(a,x)$ decreases when t increases. For $x \simeq 0$ the second terms are noticeable because, when $x << 2\sqrt{a}$ $(t << 1)$

$$M(a,x) \sim \exp(-\sqrt{a}x)\beta(a)^{-1}\ ; \tag{38}$$

contrary, when $a = 0$, $M(0,x) = \frac{1}{\sqrt{2}}e^{-x^2/2}$ and for moderately large x the second terms can be neglected.

For negative a, we rewrite the expansions (2.14) and (2.19) in [12] as:

$$\begin{aligned} \widetilde{V}(a,x) &= \frac{1}{\sqrt{\pi}}\left(\frac{x^2}{4}+a\right)^{-1/4} P_a\, , \\ \widetilde{V}'(a,x) &= \frac{1}{\sqrt{\pi}}\left(\frac{x^2}{4}+a\right)^{1/4} Q_a\, . \end{aligned} \tag{39}$$

These representations are the same as in Eq. (34) except that the second terms have disappeared.

The unscaled functions can be obtained by multiplying (28) or dividing (34) and (39) by $F(a,x)$ (Eq. (13)).

6.2 Case $a << 0$, $0 \leq x < 2\sqrt{-a}$ (oscillatory region)

In the oscillatory region, we use the asymptotic expansions given by Olver [10], which are valid for large $|a|$ uniformly with respect to $|t| \leq 1-\epsilon$, ϵ being a small positive number. The expansions for the scaled functions are given by

$$
\begin{aligned}
\widetilde{U}(a,x) &= \frac{\sqrt{2}}{\lambda(x,a)} G(\mu)[C_1(a,x)\cos\phi(a,x) + S_1(a,x)\sin\phi(a,x)]\,,\\
\widetilde{U'}(a,x) &= \sqrt{2}\lambda(x,a)G(\mu)[-S_2(a,x)\sin\phi(a,x) + C_2(a,x)\cos\phi(a,x)]\,,\\
\widetilde{V}(a,x) &= \frac{1}{\sqrt{\pi}\lambda(x,a)}\beta(|a|)G(\mu)[C_1(a,x)\sin\phi(a,x) - S_1(a,x)\cos\phi(a,x)]\,, \qquad (40)\\
\widetilde{V'}(a,x) &= \frac{1}{\sqrt{\pi}}\lambda(x,a)\beta(|a|)G(\mu)[S_2(a,x)\cos\phi(a,x) + C_2(a,x)\sin\phi(a,x)]\,,
\end{aligned}
$$

where

$$\lambda(x,a) = \left|\frac{x^2}{4} + a\right|^{1/4}\,, \qquad (41)$$

$$\phi(a,x) = -\mu^2\eta + \tfrac{1}{4}\pi = 2a\eta + \pi/4\,, \qquad (42)$$

η is defined in Eq. (10), $\beta(|a|)$ is given by Eq. (21) and $G(\mu)$ is given later (Eq. (49)) in the form of an asymptotic expansion.

Similarly as in the non-oscillatory case, when $|a|$ is large both the numerator and the denominator of $\beta(|a|)$ will overflow. In this case, the following expressions are preferable for the $V-$functions [10]:

$$
\begin{aligned}
\widetilde{V}(a,x) &= \frac{1}{\sqrt{\pi}\lambda(x,a)G(\mu)S(\mu)}[C_1(a,x)\sin\phi(a,x) - S_1(a,x)\cos\phi(a,x)]\,,\\
\widetilde{V'}(a,x) &= \frac{\lambda(x,a)}{\sqrt{\pi}G(\mu)S(\mu)}[S_2(a,x)\cos\phi(a,x) + C_2(a,x)\sin\phi(a,x)]\,, \qquad (43)
\end{aligned}
$$

where $\beta(|a|)$ in Eq. (40) can be written as

$$\beta(|a|) = \frac{1}{G(\mu)^2 S(\mu)}, \qquad (44)$$

and the quantities $G(\mu)$, $S(\mu)$, $S_i(a,x)$ and $C_i(a,x)$, $i = 1,2$, are available in the form of asymptotic expansions.

We have

$$
\begin{aligned}
C_1(a,x) &\sim \sum_{s=0}^{\infty} \frac{(-1)^s u_{2s}(t)}{(1-t^2)^{3s}\mu^{4s}}\,, & S_1(a,x) &\sim \sum_{s=0}^{\infty} \frac{(-1)^s u_{2s+1}(t)}{(1-t^2)^{3s+3/2}\mu^{4s+2}}\,,\\
C_2(a,x) &\sim \sum_{s=0}^{\infty} \frac{(-1)^s v_{2s+1}(t)}{(1-t^2)^{3s+3/2}\mu^{4s+2}}\,, & S_2(a,x) &\sim \sum_{s=0}^{\infty} \frac{(-1)^s v_{2s}(t)}{(1-t^2)^{3s}\mu^{4s}}\,.
\end{aligned} \qquad (45)
$$

The coefficients $u_s(t)$ satisfy the relation

$$(t^2-1)u_s'(t)-3stu_s(t)=r_{s-1}(t)\,,\quad s=1,2,3\ldots, \tag{46}$$

where $u_0(t)=1$, $r_{-1}=0$, and for $s=0,1,2,\ldots$

$$8r_s(t)=(3t^2+2)u_s(t)-12(s+1)tr_{s-1}(t)+4(t^2-1)r_{s-1}'(t). \tag{47}$$

The coefficients $v_s(t)$ are given by $v_0(t)=1$ and

$$v_s(t)=u_s(t)+\frac{1}{2}tu_{s-1}(t)-r_{s-2}(t),\quad s=1,2,3,\ldots. \tag{48}$$

The asymptotic expansion for $G(\mu)$ reads:

$$G(\mu)\sim\left(\sum_{s=0}^{\infty}\frac{g_s}{\mu^{2s}}\right)^{-1}, \tag{49}$$

where

$$\mu=\sqrt{2|a|} \tag{50}$$

and

$$g_s=\lim_{t\to\infty}\frac{u_s(t)}{(t^2-1)^{3s/2}}\,. \tag{51}$$

The even coefficients are zero and the first four odd g_s coefficients are: $g_0=1$, $g_1=1/24$, $g_3=-2021/207360$, $g_5=5149591/418037760$.

$$S(\mu)\sim\sum_{k=0}^{\infty}\frac{w_k}{\mu^{4k}}\,. \tag{52}$$

The first four values of w_k are $w_0=1$, $w_1=-1/576$, $w_2=2021/2488320$, $w_3=-337566547/300987187200$.

6.3 Modulus and phase

Eq. (40) shows that when $a<<0$ and t is fixed the functions U and V become highly oscillatory. Unavoidably, relative accuracy is lost near the zeros of the functions $\widetilde{U}$, $\widetilde{U'}$, $\widetilde{V}$ and $\widetilde{V'}$ when fixed precision arithmetic is used. In addition, accuracy degrades as larger values of $|a|$ are considered. This loss of precision is related to the fact that in Eq. (40) the argument of the trigonometric functions become large as a gets larger for fixed t.

It is possible to define quantities which do not suffer from this degradation, if computed in an stable way, and to confine the error caused to a simple function. We define the moduli as:

$$\begin{aligned}M_1(a,x)&=\sqrt{\widetilde{U}(a,x)^2+2\pi\left(\frac{\tilde{V}(a,x)}{\beta(|a|)}\right)^2}\,,\\ M_2(a,x)&=\sqrt{\widetilde{U'}(a,x)^2+2\pi\left(\frac{\tilde{V}'(a,x)}{\beta(|a|)}\right)^2}\end{aligned} \tag{53}$$

and the phase functions as:

$$
\begin{aligned}
\psi_1(a,x) &= \arctan\left(\frac{\sqrt{2\pi}\,\widetilde{V}(a,x)}{\beta(|a|)\widetilde{U}(a,x)^2}\right) - \phi(a,x)\,,\\
\psi_2(a,x) &= \arctan\left(\frac{\sqrt{2\pi}\,\widetilde{V'}(a,x)}{\beta(|a|)\widetilde{U'}(a,x)^2}\right) - \phi(a,x)\,,
\end{aligned} \tag{54}
$$

where $\phi(a,x)$ is given by Eq. (42). Notice that $\phi \to -\infty$ as $a \to -\infty$, which causes errors in the evaluation of trigonometric functions for large $|a|$.

With these definitions we have

$$
\begin{aligned}
\widetilde{U}(a,x) &= G(\mu)M_1(a,x)\cos(\psi_1(a,x))\,,\\
\widetilde{U'}(a,x) &= G(\mu)M_2(a,x)\cos(\psi_2(a,x))\,,\\
\widetilde{V}(a,x) &= \frac{1}{\sqrt{2\pi}}\beta(|a|)G(\mu)M_1(a,x)\sin(\psi_1(a,x))\,,\\
\widetilde{V'}(a,x) &= \frac{1}{\sqrt{2\pi}}\beta(|a|)G(\mu)M_2(a,x)\cos(\psi_2(a,x))\,.
\end{aligned} \tag{55}
$$

The moduli M_1 and M_2 do not suffer from error degradation for large $|a|$ in the oscillatory region when the expressions in Eq. (55) or Eqs. (40) and (43) are used. This is trivially true because $\cos^2\psi + \sin^2\psi = 1$ for any phase function ψ, no matter if ψ is very large and the $\sin\psi$ and $\cos\psi$ values are completely inaccurate (however, it is not *numerically true* that $\cos^2\psi + \cos^2(\psi - \pi/2) = 1$ for large ψ).

7. AIRY-TYPE ASYMPTOTIC EXPANSIONS

When $a << 0$, $x \geq 0$, Airy-type uniform asymptotic expansions are given in [10] (see also Section 3 of ([12]). Here we provide expressions for the scaled functions.

For large a in the monotonic region $a > -x^2/4$, and for computing scaled PCFs, it is convenient to absorb the remaining exponential factor in the Airy-type asymptotic expansions for the scaled PCFs by using scaled Airy functions [5] instead of plain Airy functions (when their argument is positive). Indeed, this exponential factor tends to cancel the dominant exponential of the plain Airy functions, causing large rounding errors. Also overflow/underflow errors take place. Therefore, for a stable computation, the accurate evaluation of scaled Airy functions of positive argument is needed. In [7], a Fortran 90 version of the code by Fullerton [4] is used (the Fortran 77 code is available at Netlib). Algorithm 819 [5], which computes Airy functions in the complex plane is also available, although for real computations an approach based on Chebyshev approximations is more efficient. Also, we find that for fixed precision the Chebyshev approach is more efficient that the method considered in [3], which is partly based on the integration of the defining second order ODE (see also [2]).

With the usual notation $\mu = \sqrt{2|a|}$ and $t = x/(2\sqrt{|a|})$, for the scaled U-functions the expansions in terms of the scaled Airy functions read:

$$
\widetilde{U}(a,x) = 2^{3/4}\pi^{1/2}\mu^{-1/6}G(\mu)\phi(\zeta)\left[\widehat{\mathrm{Ai}}(\mu^{4/3}\zeta)A_\mu(\zeta) + \frac{\widehat{\mathrm{Ai}'}(\mu^{4/3}\zeta)}{\mu^{8/3}}B_\mu(\zeta)\right]\,, \tag{56}
$$

$$\widetilde{U'}(a,x)=2^{1/4}\pi^{1/2}\mu^{1/6}\frac{G(\mu)}{\phi(\zeta)}\left[\frac{\widehat{\rm Ai}(\mu^{4/3}\zeta)}{\mu^{4/3}}C_\mu(\zeta)+\widehat{\rm Ai'}(\mu^{4/3}\zeta)D_\mu(\zeta)\right]. \qquad (57)$$

For the $V-$functions, an alternative expression for the front factors to that in [10] and [12] can be used which is better suited for large a, similarly as done in Section 6.2 for the expansions in terms of elementary functions. Namely:

$$\widetilde{V}(a,x)=2^{1/4}\mu^{-1/6}\frac{\phi(\zeta)}{G(\mu)S(\mu)}\left[\widehat{\rm Bi}(\mu^{4/3}\zeta)A_\mu(\zeta)+\frac{\widehat{\rm Bi'}(\mu^{4/3}\zeta)}{\mu^{8/3}}B_\mu(\zeta)\right], \qquad (58)$$

$$\widetilde{V'}(a,x)=2^{-1/4}\mu^{1/6}\frac{1}{G(\mu)S(\mu)\phi(\zeta)}\left[\frac{\widehat{\rm Bi}(\mu^{4/3}\zeta)}{\mu^{4/3}}C_\mu(\zeta)+\widehat{\rm Bi'}(\mu^{4/3}\zeta)D_\mu(\zeta)\right], \qquad (59)$$

where $G(\mu)$ is given by Eq. (49), $S(\mu)$ is given by Eq. (52). $\widehat{\rm Ai}(x)$, $\widehat{\rm Ai'}(x)$, $\widehat{\rm Bi}(x)$, $\widehat{\rm Bi'}(x)$ are scaled Airy functions [5] for positive x and plain Airy functions for negative x. This means that, for $x>0$

$$\begin{aligned}\widehat{\rm Ai}(x)=e^{\frac{2}{3}x^{3/2}}{\rm Ai}(x)\,,\quad \widehat{\rm Ai'}(x)=e^{\frac{2}{3}x^{3/2}}{\rm Ai}'(x)\,,\\ \widehat{\rm Bi}(x)=e^{-\frac{2}{3}x^{3/2}}{\rm Bi}(x)\,,\ \widehat{\rm Bi'}(x)=e^{-\frac{2}{3}x^{3/2}}{\rm Bi}'(x)\,,\end{aligned} \qquad (60)$$

while $\widehat{\rm Ai}(x)={\rm Ai}(x)$ when $x<0$ and the same is true for the derivative and for ${\rm Bi}(x)$ and its derivative.

The parameter ζ is defined as $\zeta=\frac{3}{2}\Theta^{2/3}$ with Θ as given in Eq. (10) and the values are taken in the principal branch. As a function of t

$$\begin{aligned}&\frac{2}{3}(-\zeta)^{3/2}=\tfrac{1}{2}\arccos(t)-\tfrac{1}{2}t\sqrt{1-t^2}\,,\ -1<t\le 1\,,(\zeta\le 0)\,,\\ &\frac{2}{3}(\zeta)^{3/2}=\tfrac{1}{2}t\sqrt{t^2-1}-\tfrac{1}{2}\log(t+\sqrt{t^2-1})\,,\ t\ge 1\ ,\,(\zeta\ge 0)\,.\end{aligned} \qquad (61)$$

In addition

$$\phi(\zeta)=\left(\frac{\zeta}{t^2-1}\right)^{1/4}, \qquad (62)$$

$$\begin{aligned}A_\mu(\zeta)\sim\sum_{s=0}^{\infty}\frac{a_s(\zeta)}{\mu^{4s}}\,,\qquad B_\mu(\zeta)\sim\sum_{s=0}^{\infty}\frac{b_s(\zeta)}{\mu^{4s}}\,,\\ C_\mu(\zeta)\sim\sum_{s=0}^{\infty}\frac{c_s(\zeta)}{\mu^{4s}}\,,\qquad D_\mu(\zeta)\sim\sum_{s=0}^{\infty}\frac{d_s(\zeta)}{\mu^{4s}}\,.\end{aligned} \qquad (63)$$

The coefficients $a_s(\zeta)$ and $b_s(\zeta)$ are computed through the expansions

$$a_s(\zeta)=\sum_{t=0}^{\infty}a_s^t\eta^t\,,\ b_s(\zeta)=2^{1/3}\sum_{t=0}^{\infty}b_s^t\eta^t\,, \qquad (64)$$

where $\eta = 2^{-1/3}\zeta$.

The coefficients $c_s(\zeta)$ and $d_s(\zeta)$ are given by

$$c_s(\zeta) = \chi(\zeta)a_s(\zeta) + a_s'(\zeta) + \zeta b_s(\zeta)\,,\ d_s(\zeta) = a_s(\zeta) + \chi(\zeta)b_{s-1}(\zeta) + b_{s-1}'(\zeta)\,, \quad (65)$$

where

$$\chi(\zeta) = \frac{1 - 2t[\phi(\zeta)]^6}{4\zeta}\,. \quad (66)$$

When t is close to 1 (ζ close to 0) it is better to compute the functions $\phi(\zeta)$ and $\chi(\zeta)$ through the expansions

$$\phi(\zeta) = 2^{-1/6}\sum_{k=0}^{\infty} f_k\eta^k\,, \quad \chi(\zeta) = 2^{-1/3}\sum_{k=0}^{\infty} h_k\eta^k\,. \quad (67)$$

8. RECURRENCE RELATIONS

PCFs verify the following recurrence relations

$$U(a-1,x) = xU(a,x) + \left(a + \tfrac{1}{2}\right)U(a+1,x)\,, \quad (68)$$

and

$$V(a+1,x) = xV(a,x) + \left(a - \tfrac{1}{2}\right)V(a-1,x). \quad (69)$$

We also have the following relation for the derivatives:

$$\begin{aligned} U'(a,x) &= -\tfrac{1}{2}x\,U(a,x) - \left(a + \tfrac{1}{2}\right)U(a+1,x)\,, \\ V'(a,x) &= \tfrac{1}{2}x\,V(a,x) + \left(a - \tfrac{1}{2}\right)V(a-1,x)\,. \end{aligned} \quad (70)$$

It is easy to check that the recurrence for the U function in Eq. (68) has as a second solution the V function multiplied by a factor not depending on x and a similar situation happens for the recurrence for the V function, Eq. (69). Exceptions are the negative semi-integer values for the U-recurrence and positive semi-integer values for the V-recurrence, as we will later discuss.

We can take as linearly independent pair of solutions of (68):

$$\{y_1(a), y_2(a)\} \equiv \{U(a,x), e^{i\pi a}V(a,x)/\Gamma(a+\tfrac{1}{2})\} \quad (71)$$

for positive a and for negative a but $a \neq -k + 1/2$, $k \in \mathbb{N}$. Let us notice that in the case $a = -k + 1/2$, $k \in \mathbb{N}$, the recurrence has only one linearly independent solution. Indeed, setting $a = -1/2$ in Eq. (68), we have the constraint $U(-3/2,x) = xU(-1/2,x)$ and then all the sequences verifying the recurrence are necessarily of the form $CU(-k+1/2,x)$ with C a constant. It is then advisable not to use this recurrence for computing $V(a,x)/\Gamma(a+1/2)$ values, particularly near negative semi-integer values of a.

For this recurrence and for $a \to +\infty$ it is easy to check from the asymptotic expansions previously discussed that $U(a,x)$ is a minimal solution because $\lim_{a\to+\infty} y_1(a)/y_2(a) = 0$. Indeed, from (28) and (34) we see that

$$|y_1(a)/y_2(a)| = |\Gamma(a+\tfrac{1}{2})U(a,x)/V(a,x)| \sim \pi \exp(-2\sqrt{a}x)\,. \tag{72}$$

Therefore, $U(a,x)$ is minimal for $x>0$ as $a \to +\infty$. This means that, for positive a, recursion for $U(a,x)$ ($V(a,x)$) is only stable in the backward (forward) direction, that is, for decreasing (increasing) a.

As $a \to -\infty$ for fixed x the situation is quite different. Let us, for instance, consider the recurrence relation (69), which is satisfied by the following pair of independent solutions for negative a:

$$\{w_1(a), w_2(a)\} \equiv \{V(a,x), U(a,x)/\Gamma(\tfrac{1}{2}-a)\}\,. \tag{73}$$

This is also a linearly independent pair of solution of the recurrence for positive a but $a \neq -1/2+k$, $k \in \mathbb{N}$.

Considering Eq. (40) we see that, as $a \to -\infty$:

$$w_2(a) = U(a,x)/\Gamma(1/2-a) \sim \frac{1}{\sqrt{\pi}}(-a)^{a/2-1/4}e^{-a/2}\cos\phi(a,x)\,, \tag{74}$$

where $\phi(a,x) \sim a\pi/2 + \pi/4$ and

$$w_1(a) = V(a,x) \sim \frac{1}{\sqrt{\pi}}(-a)^{a/2-1/4}e^{-a/2}\sin\phi(a,x)\,. \tag{75}$$

Therefore any solution of (69) has the asymptotic behavior

$$y(a) \sim C(-a)^{a/2-1/4}e^{-a/2}\sin(\phi(a,x)+\Phi) \tag{76}$$

for some constants C and Φ. Clearly, no minimal solution exists as $a \to -\infty$ for fixed x. This means that recursion is well conditioned in both directions for negative values of a in the oscillatory region $x^2/4 + a < 0$ and for any solution of the three term recurrence. Only the usual accumulation of rounding errors will take place in this case.

However, it is important to note that the behavior of the solutions for negative a in the non-oscillatory region $x^2/4 + a > 0$ is similar to the behavior for positive a, particularly for not too small x. Indeed, considering a large fixed value of x, we have that for large enough $|a|$ in the oscillatory region ($a < -x^2/4$) the solutions $w_1(a)$ and $w_2(a)$ are of the same size, but, when $|a| << x$, $w_1(x)$ is much larger (exponentially) than $w_2(a)$ (Eq. (4)); then, we infer that $w_1(a)/w_2(a)$ will increase for increasing values of a ($a < 0$) in the non-oscillatory region. This can also be checked by considering the uniform asymptotic expansions in terms of elementary functions. As $a \to -\infty$ in the monotonic region we have

$$r(a) \equiv \frac{w_1(a)}{w_2(a)} \sim 2e^{-4a\xi}\,, \tag{77}$$

with ξ as given in Eq. (10). The ratio $r(a)$ shows a steep increase as a increases, particularly when x is large; indeed $dr/da = 4\log(t+\sqrt{t^2-1})e^{-4a\xi} > 0$. As a consequence, only if the a-values are inside the oscillatory region, both solutions can be safely computed in both directions.

In summary, the U-recurrence (68) can be used to compute values of $U(a,x)$ in the backward direction (a decreasing). It can also be used in the forward direction for values of a such that $a < -x^2/4$. On the other hand, the V-recurrence (69) can always be used in the forward direction, while the backward direction is also possible for values of a verifying $a < -x^2/4$.

9. COMPUTATION THROUGH INTEGRAL REPRESENTATIONS

The algorithms are based on non-oscillating integral representations which are obtained by using methods from asymptotic analysis. A detailed study of how these stable integral representations are obtained can be found in [6]. Our algorithms follow the main results given in this reference. In the next sections, we give details on the paths used for computing the integrals in each parameter region and on the selection of the quadrature rules. Following [9], we will consider the application of the trapezoidal rule with a suitable change of the integration variable (in particular, we will use the **erf**-rule).

9.1 Computing for $a > 0,\ x \geq 0$

For $a > 0$ we compute $V(a,x)$ from the Eq. (33). We evaluate $U(a,x)$ and $U(a,-x)$, $a > 0$, from stable integral representations.

9.1.1 *$U(a,x)$ and $U'(a,x)$ for $a > 0$, $x \geq 0$.* The starting point is the integral representation for $U(a,x)$

$$U(a,x) = \frac{e^{\frac{1}{4}x^2}}{i\sqrt{2\pi}} \int_{\mathcal{C}} e^{-xs+\frac{1}{2}s^2} s^{-a} \frac{ds}{\sqrt{s}}, \tag{78}$$

where $\mathcal{C}$ is a vertical line on which $\Re s > 0$.

The positive saddle point of the integrand is given by

$$w_0 = t + \sqrt{t^2+1}\,, \quad t = \frac{x}{2\sqrt{a}}\,. \tag{79}$$

Let us integrate (78) along the vertical through w_0. We obtain

$$\widetilde{U}(a,x) = \frac{a^{1/4}}{\sqrt{2\pi}} \int_{-\infty}^{\infty} e^{-a\psi(v)} \frac{dv}{\sqrt{w_0+iv}} \equiv \frac{a^{1/4}}{\sqrt{2\pi}} I(a,x)\,, \tag{80}$$

where

$$\psi(v) = \tfrac{1}{2}v^2 + \tfrac{1}{2}\ln(1+v^2/w_0^2) + i\left[(2t-w_0)v + \arctan(v/w_0)\right]. \tag{81}$$

By replacing $v \to v w_0$, we obtain

$$I(a,x) = \sqrt{w_0} \int_{-\infty}^{\infty} e^{-a\psi(v)} \frac{dv}{\sqrt{1+iv}}\,, \tag{82}$$

where now

$$\psi(v) = \tfrac{1}{2}v^2(w_0^2+1) + \tfrac{1}{2}\left[\ln(1+v^2) - v^2\right] + i\left[\arctan(v) - v\right]. \tag{83}$$

Next we take $v = \sigma p$, where $\sigma = \sqrt{2/[a(w_0^2+1)]}$, to remove a and t (or x) from the dominant part in the exponential function. This gives

$$I(a,x) = \sigma\sqrt{w_0}\int_{-\infty}^{\infty} e^{-\psi(p)}\frac{dp}{\sqrt{1+iv}}. \tag{84}$$

where now

$$\psi(p) = p^2 + \tfrac{1}{2}a\left[\ln(1+v^2) - v^2\right] + ia\left[\arctan(v) - v\right] = \psi_r(p) + i\psi_i(p). \tag{85}$$

We separate the real and imaginary parts:

$$I(a,x) = \sigma\sqrt{w_0}\int_{-\infty}^{\infty} e^{-\psi_r(p)}[\cos\chi + i\sin\chi]\frac{dp}{(1+v^2)^{\frac{1}{4}}}, \tag{86}$$

where the imaginary part of the integrand is odd (and vanishes), and

$$\chi = -\psi_i(p) - \tfrac{1}{2}\arctan(v). \tag{87}$$

The real part is even, and we reduce the domain of integration to $[0,\infty)$. To get a finite integral, we replace the upper limit by p_0. Next, in order to get an integral suitable for application of the trapezoidal rule (as explained in [9]), we substitute $p = p_0\mathrm{erf}(r)$, where erf is the error function defined by

$$\mathrm{erf}\, z = \frac{2}{\sqrt{\pi}}\int_0^z e^{-t^2}\, dt. \tag{88}$$

This gives

$$I(a,x) = 4p_0\sigma\sqrt{w_0}\frac{1}{\sqrt{\pi}}\int_0^{\infty} e^{-r^2}e^{-a\psi_r(p)}\cos\chi\frac{dr}{(1+v^2)^{\frac{1}{4}}}. \tag{89}$$

For the derivative we have

$$\widetilde{U'}(a,x) = -\frac{a^{3/4}}{\sqrt{2\pi}}I_d(a,x)\,, \tag{90}$$

where

$$I_d(a,x) = 2p_0\sigma\sqrt{\frac{w_0}{a}}\int_{-\infty}^{\infty} e^{-r^2}e^{-a\psi_r(p)}e^{i\chi}[\sqrt{t^2+1} + iw_0v]\frac{dr}{(1+v^2)^{\frac{1}{4}}}. \tag{91}$$

The imaginary part of the integrand is odd and vanishes, the real part is even, and we have

$$I_d(a,x) = 8p_0\sigma\sqrt{\frac{w_0}{a}}\int_0^{\infty} e^{-r^2}e^{-a\psi_r(p)}[\sqrt{t^2+1}\cos\chi - w_0v\sin\chi]\frac{dr}{(1+v^2)^{\frac{1}{4}}}. \tag{92}$$

We choose an upper limit (b_0) of the $r-$integrals in (89) and (92), which can be estimated from the expression $\exp(-b_0^2) = \varepsilon/10$.

On the other hand, the upper limit p_0 follows from neglecting the logarithm in $\psi_r(p)$. Then, we estimate p_0 from the equation

$$e^{-p_0^2w_0^2/(w_0^2+1)} = \varepsilon/10\,, \tag{93}$$

where ε is the precision demanded in the computation of the functions.

For the $p-$integral this value is quite realistic. In the $r-$integral the damping factor of $\exp(-r^2)$ makes this value too large. However, at several moments in the implementation of the trapezoidal rule, a check is performed to avoid too many evaluations.

9.1.2 *$U(a,-x)$ and $U'(a,-x)$ for $a>0$, $x\geq 0$.* For computing the $V(a,x)$ function and its derivative for $a>0$ and $x\geq 0$, we will use Eq. (33). For this, we need to compute $U(a,-x)$ and $U'(a,-x)$ for $a>0$, $x\geq 0$.

We define

$$U(a,-x)=\frac{a^{\frac14}\sqrt{w_0}F(a,x)}{\Gamma(a+\frac12)}\,J(a,x), \tag{94}$$

$$U'(a,-x)=-\frac{a^{\frac34}\sqrt{w_0}F(a,x)}{\Gamma(a+\frac12)}\,J_d(a,x), \tag{95}$$

and using Eqs. (2.21), (2.23) of [6] we have:

$$\begin{aligned} J(a,x) &= \int_{-1}^{\infty} e^{-a\psi(u)}\,\frac{du}{\sqrt{1+u}}, \\ J_d(a,x) &= \int_{-1}^{\infty} e^{-a\psi(u)}\,\left(\sqrt{t^2+1}+w_0u\right)\frac{du}{\sqrt{1+u}}\,, \end{aligned} \tag{96}$$

where

$$\psi(u)=\tfrac12 w_0^2u^2+u-\ln(1+u)\,. \tag{97}$$

If we write $u=\sigma p$, $\sigma=\sqrt{2/(aw_0^2)}$, we obtain

$$J(a,x)=\sigma\int_{-1/\sigma}^{\infty} e^{-\psi(p)}\,\frac{dp}{\sqrt{1+u}}, \tag{98}$$

where now

$$\psi(p)=p^2+a[u-\ln(1+u)]. \tag{99}$$

A finite interval is obtained by replacing the upper limit by a finite value b_0. Because $\psi(p)\geq p^2$ we take for b_0 the number that is used in the $r-$integrals (89) and (92). Next the finite interval $[-1/\sigma,b_0]$ is transformed into $[-1,1]$ by writing

$$p=\frac{q}{q_0+q_1q},\quad q_0=\frac{1+\sigma b_0}{2b_0},\quad q_1=\frac{1-\sigma b_0}{2b_0}. \tag{100}$$

This keeps the origin at the saddle point, and we obtain

$$J(a,x)=\sigma\int_{-1}^{1} e^{-\psi(p)}\,\frac{dp}{dq}\frac{dq}{\sqrt{1+u}}. \tag{101}$$

Finally we substitute $q=\operatorname{erf}(r)$, which gives

$$J(a,x)=\frac{2\sigma}{\sqrt{\pi}}q_0\int_{-\infty}^{\infty} e^{-r^2}e^{-\psi(p)}\,\frac{1}{(q_0+q_1q)^2}\frac{dr}{\sqrt{1+u}}. \tag{102}$$

We proceed similarly with $J_d(a,x)$:

$$J_d(a,x) = \frac{2\sigma}{\sqrt{\pi}} q_0 \int_{-\infty}^{\infty} e^{-r^2} e^{-\psi(p)} \frac{1}{(q_0+q_1 q)^2} [\sqrt{t^2+1} + w_0 u] \frac{dr}{\sqrt{1+u}}. \qquad (103)$$

In the algorithm [7] the interval $[-\infty, \infty]$ is reduced to $[0, \infty]$ by combining odd and even parts of the $r-$integrand. The upper limit is replaced by r_0 obtained from the equation $e^{-r_0^2} = \varepsilon/10$.

9.1.3 *Wronskian relation for the integrals.* From the Wronskian relation between $U(a,x)$ and $U(a,-x)$

$$\mathcal{W}[U(a,x), U(a,-x)] = \frac{\sqrt{2\pi}}{\Gamma(a+\frac{1}{2})}, \qquad (104)$$

we obtain the relation for the integrals:

$$I(a,x)\, J_d(a,x) + I_d(a,x)\, J(a,x) = \frac{2\pi}{a\sqrt{w_0}}. \qquad (105)$$

It is convenient to combine the computation of $U(a,x)$ with that of $U(a,-x)$ because of two main reasons:

(1) When computing the four quantities $I(a,x), J(a,x), I_d(a,x), J_d(a,x)$ in one algorithm the Wronskian relation (105) can be used for a stopping criterion.

(2) The time needed for the evaluation of the error function is cut down to a minimum.

9.1.4 *Scaled functions $a > 0,\ x \geq 0$.* By considering Eqs. (80), (90), (94), (95) and (33) the computation of the scaled functions can be summarized as follows.

The scaled U-functions read

$$\widetilde{U}(a,x) = \frac{a^{1/4}}{\sqrt{2\pi}} I(a,x)\,,\ \widetilde{U'}(a,x) = -\frac{a^{3/4}}{\sqrt{2\pi}} I_d(a,x)\,, \qquad (106)$$

where $I(a,x)$ and $I_d(a,x)$ are computed by means of Eqs. (89) and (92).

For the $V-$functions the scaling reads

$$\begin{aligned} \widetilde{V}(a,x) &= \frac{a^{1/4}}{\pi} \left[\sqrt{w_0} J(a,x) + \sin \pi a M(a,x) I(a,x)\right], \\ \widetilde{V'}(a,x) &= \frac{a^{3/4}}{\pi} \left[\sqrt{w_0} J_d(a,x) - \sin \pi a M(a,x) I_d(a,x)\right], \end{aligned} \qquad (107)$$

where $M(a,x)$, as defined in Eq. (35). The same precautions regarding underflow described in section 6.1 should be considered now.

$J(a,x)$ and $J_d(a,x)$ are computed by means of Eqs. (102) and (103).

9.2 Computing for $a < 0,\ x \geq 0$

As before, we define $t = x/(2\sqrt{|a|})$. We will consider separately the monotonic case $t > 1$, the oscillatory case $0 \leq t < 1$ and the oscillatory case near the turning points $t \lesssim 1$.

9.2.1 *Oscillatory region: $a < 0$ and $0 \le t < 1$.* Our starting point in this case is the following integral representation for the function $Y(-a,x)$, $\Re a < 1/2$:

$$Y(-a,x) = (-a)^{-a/2+1/4} \int_0^\infty e^{a\phi(w)} \frac{dw}{\sqrt{w}}, \tag{108}$$

where

$$\phi(w) = \tfrac{1}{2}w^2 - 2itw - \ln w. \tag{109}$$

The function $Y(-a,x)$ is related to $U(a,x)$ and $V(a,x)$ through the following equation

$$\sqrt{\tfrac{2}{\pi}} e^{i\frac{\pi}{2}(a+\frac{1}{2})} e^{\frac{1}{4}x^2} Y(-a,x) = U(a,x) + i\Gamma\left(\tfrac{1}{2} - a\right) V(a,x). \tag{110}$$

We see that $U(a,x)$ and $V(a,x)$, $a < 0$, can be obtained by considering the real and imaginary parts of (108).

In [6] it was shown that an approximation to the steepest descent path for the integral (108) is given by $w = u + iv$ with

$$v = \frac{ut(1+u_+)}{u+u_+^2}, \quad u_+ = \sqrt{1-t^2}, \quad t = \frac{x}{2\sqrt{|a|}}. \tag{111}$$

The path of steepest descent follows from solving the equation

$$\Im\phi(w) = \Im\phi(w_+), \tag{112}$$

where $w_+ = it + \sqrt{1-t^2}$ is a saddle point and

$$\phi(w_+) = \tfrac{1}{2} + t^2 + 2i\left(\eta - \tfrac{1}{4}\pi\right), \quad \eta = \tfrac{1}{2}\left(\arccos t - t\sqrt{1-t^2}\right). \tag{113}$$

The path (111) runs through the saddle point $w_+ = u_+ + iw_+$, and has the same slope at this point as the exact steepest descent path.

As remarked in Section 3.1 of [6], this path becomes non-smooth when t approaches 1. A reasonable interval range for the application of the integral representations considered in this section is $0 \le t \le 0.9$. Specific integral representations for the case $t \sim 1$ will be considered in a later section.

We integrate (108) with respect to u, using (111) for the corresponding values of v. We write $p = u - u_+, q = v - v_+$ and integrate with respect to p. This gives

$$Y(-a,x) = \frac{j(a,x)}{\sqrt{w_+}} \int_{-u_+}^\infty e^{a\psi(p)} \left(1 + i\frac{dq}{dp}\right) \frac{dp}{\sqrt{1+\zeta}}, \tag{114}$$

where

$$j(a,x) = (-a)^{-a/2+1/4} e^{a\phi(w_+)}, \tag{115}$$

$$\psi(p) = \frac{1}{2}(p+iq)^2 - \left[\ln(1+\zeta) - \zeta\right], \tag{116}$$

and

$$\zeta = \frac{p+iq}{w_+},\ q = \frac{p_0 p}{p+p_1},\ p_0 = u_+ v_+,\ p_1 = u_+ + u_+^2,\ \frac{dq}{dp} = \frac{p_0 p_1}{(p+p_1)^2}. \tag{117}$$

We use an auxiliary algorithm for the evaluation of $\ln(1+z)-z$ for small complex z. This can be done by using a Taylor series, or by using auxiliary functions for the real case. In the latter approach one has, with $z=\kappa+i\tau$, $\kappa>-1$,

$$\ln(1+z)-z = \tfrac{1}{2}[\ln(1+\xi)-\xi] + \tfrac{1}{2}(\kappa^2+\tau^2) + i\left\{[\arctan\eta - \eta] - \kappa\eta\right\}, \tag{118}$$

where

$$\xi = 2\kappa+\kappa^2+\tau^2, \quad \eta = \frac{\tau}{1+\kappa}. \tag{119}$$

Take $p=\sigma r$, $\sigma=\sqrt{2/|a|}$, and take r_0 as the upper limit in the new integral. A first estimate of r_0 is obtained from the equation $e^{-r_0^2}=\varepsilon/10$. This gives

$$Y(-a,x) \simeq \sigma\frac{j(a,x)}{\sqrt{w_+}}\int_{-u_+/\sigma}^{r_0} e^{a\psi(p)}\left(1+i\frac{dq}{dp}\right)\frac{dr}{\sqrt{1+\zeta}}. \tag{120}$$

The finite interval $[-u_+/\sigma, r_0]$ is transformed to $[-1,1]$ by writing

$$r = \frac{s}{s_0+s_1 s}, \quad s_0 = \frac{u_+ + \sigma r_0}{2u_+ r_0}, \quad s_1 = \frac{u_+ - \sigma r_0}{2u_+ r_0}, \quad \frac{dr}{ds} = \frac{s_0}{(s_0+s_1 s)^2}. \tag{121}$$

Finally, this integral is transformed by using $s=\operatorname{erf}\rho$, and we obtain, writing $\psi(p)=\psi_r(p)+i\psi_i(p)$,

$$Y(-a,x) \simeq \frac{2\sigma}{\sqrt{\pi}}\frac{j(a,x)}{\sqrt{w_+}}\int_{-\infty}^{\infty} e^{-\rho^2+a\psi_r(p)}\frac{dr}{ds}g(\rho)\,d\rho, \tag{122}$$

where

$$g(\rho) = \left(1+i\frac{dq}{dp}\right)\frac{1}{\sqrt{1+\zeta}}\frac{1}{\sqrt{w_+}}. \tag{123}$$

The interval $[-\infty,\infty]$ can be reduced to $[0,\infty]$ by combining odd and even parts of the $\rho-$integrand. The upper limit is replaced by ρ_0 obtained from the equation $e^{-\rho_0^2}=\varepsilon/10$. By analogy with (3.14) and (3.23) of [6] we have

$$\begin{aligned} &U(a,x) + i\Gamma\left(\tfrac{1}{2}-a\right)V(a,x) \simeq \\ &\frac{2\sqrt{2}\sigma|a|^{1/4}}{\pi f(a)}\, e^{i(2a\eta+\frac{1}{4}\pi)} \int_{-\rho_0}^{\rho_0} e^{-\rho^2+a\psi_r(p)}\frac{dr}{ds}g(\rho)\,d\rho, \end{aligned} \tag{124}$$

$$\begin{aligned} &U'(a,x) + i\Gamma\left(\tfrac{1}{2}-a\right)V'(a,x) \simeq \\ &\frac{2\sqrt{2}\sigma|a|^{5/4}}{\pi f(a)}\, e^{i(2a\eta+\frac{1}{4}\pi)} \int_{-\rho_0}^{\rho_0} e^{-\rho^2+a\psi_r(p)}\frac{dr}{ds}h(\rho)\,d\rho, \end{aligned} \tag{125}$$

where $f(a)=(-a)^{a/2}e^{-a/2}$ and

$$h(\rho) = (t+iw)g(\rho) = [-q+i(p+u_+)]g(\rho). \tag{126}$$

We write (cf. (3.17) and (3.24) of [6])

$$g(\rho) = g_1(\rho) - i g_2(\rho), \quad h(\rho) = h_1(\rho) - i h_2(\rho). \tag{127}$$

To obtain expressions for $g_j(\rho)$, we write $t = \sin\theta$, which gives $w_+ = e^{i\theta}$. Further we write $\ln(1+\zeta) - \zeta = \alpha + i\beta$, and $\zeta = \kappa + i\tau$. Then

$$\frac{1}{\sqrt{1+\zeta}}\frac{1}{\sqrt{w_+}} = e^{-\frac{1}{2}[i\theta + \ln(1+\zeta)]} = e^{-\frac{1}{2}(\kappa+\alpha) - \frac{1}{2}i(\theta+\tau+\beta)}. \tag{128}$$

Hence,

$$g_1(\rho) = e^{-\frac{1}{2}(\kappa+\alpha)}\left[\cos\chi + \sin\chi\frac{dq}{dp}\right], \quad g_2(\rho) = e^{-\frac{1}{2}(\kappa+\alpha)}\left[\sin\chi - \cos\chi\frac{dq}{dp}\right], \tag{129}$$

where $\chi = -a\psi_i(p) + \frac{1}{2}(\theta+\tau+\beta)$.

The expressions for $U(a,x)$, $V(a,x)$, $U'(a,x)$ and $V'(a,x)$ functions written in real form are

$$\widetilde{U}(a,x) = \sqrt{\frac{2}{\pi}}|a|^{\frac{1}{4}}\left[G_1(a,x)\cos\phi(a,x) + G_2(a,x)\sin\phi(a,x)\right], \tag{130}$$

$$\widetilde{U'}(a,x) = \sqrt{\frac{2}{\pi}}|a|^{\frac{3}{4}}\left[H_1(a,x)\cos\phi(a,x) + H_2(a,x)\sin\phi(a,x)\right], \tag{131}$$

$$\widetilde{V}(a,x) = \frac{1}{\pi}|a|^{\frac{1}{4}}\beta(|a|)\left[G_1(a,x)\sin\phi(a,x) - G_2(a,x)\cos\phi(a,x)\right], \tag{132}$$

$$\widetilde{V'}(a,x) = \frac{1}{\pi}|a|^{\frac{3}{4}}\beta(|a|)\left[H_1(a,x)\sin\phi(a,x) - H_2(a,x)\cos\phi(a,x)\right], \tag{133}$$

with $\phi(a,x)$ as given in Eq.(42) and $\beta(|a|)$ was defined in Eq. (21). The integrals $G_j(a,x)$ and $H_j(a,x)$ can be computed by means of the following approximations

$$\begin{aligned} G_j(a,x) &\simeq \frac{2\sigma}{\sqrt{\pi}}\int_{-\rho_0}^{\rho_0} e^{-\rho^2 + a\psi_r(p)}\frac{dr}{ds}g_j(\rho)\,d\rho, \\ H_j(a,x) &\simeq \frac{2\sigma}{\sqrt{\pi}}\int_{-\rho_0}^{\rho_0} e^{-\rho^2 + a\psi_r(p)}\frac{dr}{ds}h_j(\rho)\,d\rho. \end{aligned} \tag{134}$$

During the computations, these four integrals can be used in the Wronskian relation

$$H_1G_2 - G_1H_2 = \frac{\pi}{|a|\beta(|a|)} = \frac{\pi}{|a|}\left[1 + \mathcal{O}\left(\frac{1}{|a|}\right)\right] \tag{135}$$

to verify if the requested precision has been obtained.

9.2.1.1 *Computing* $\psi(p)$. Using the quantities introduced earlier we have for the function $\psi(p)$ of (116):

$$\psi(p) = \tfrac{1}{2}(p^2 - q^2) + ipq - (\alpha + i\beta), \tag{136}$$

$$\alpha = \tfrac{1}{2}[\ln(1+\xi)-\xi] + \tfrac{1}{2}(\kappa^2+\tau^2), \quad \xi = 2\kappa+\kappa^2+\tau^2, \tag{137}$$

$$\beta = \arctan(\eta) - \eta - \kappa\eta, \quad \eta = \frac{\tau}{1+\kappa}, \tag{138}$$

$$\kappa = pu_+ + qv_+, \quad \tau = qu_+ - pv_+. \tag{139}$$

For small values of p the real part of $\psi(p)$ is of order p^2, unless $t \to 1$, which we exclude. For the imaginary part we have order p^3 when p is small. This is not evident from the above quantities, and some extra care is needed to obtain the correct order in a numerical computation. We have

$$\Im\psi(p) = pq + \frac{\kappa\tau}{1+\kappa} - [\arctan(\eta)-\eta]. \tag{140}$$

The first two terms are $\mathcal{O}(p^2)$, the last term is $\mathcal{O}(p^3)$. So we need to combine the first two terms. We write

$$q = \frac{p_0}{p_1}p + \mu p^2, \quad \frac{\kappa\tau}{1+\kappa} = \kappa\tau + \lambda p^3. \tag{141}$$

Then

$$\mu = -\frac{p_0}{p_1(p+p_1)}; \quad \lambda = -\frac{(1+v_+\mu p)^2(p\mu p_1 - v_+)}{(1+u_+)(1+\kappa)}. \tag{142}$$

Because

$$\frac{p_0}{p_1}p + \kappa\tau = 0, \tag{143}$$

we obtain

$$\Im\psi(p) = p^3(2u_+\mu + \lambda + u_+v_+\mu^2 p) - [\arctan(\eta)-\eta], \tag{144}$$

and this representation shows the correct behavior for small p.

9.2.2 *Oscillatory region near the transition points: $a < 0$, $t \lesssim 1$.* For values of t close or equal to 1 the approach of the previous section is not efficient. For $t \lesssim 1$ it is better to modify the method of computation, by choosing a path that remains smooth when $t \to 1$. In the algorithm [7] we use the approach described in this subsection for $0.9 \le t \le 1$.

We integrate (108) with respect to v, using $p = u - u_+, q = v - v_+$ and the path defined by

$$p = q_1 q + q_2 q^2, \quad q_1 = \frac{1+u_+}{v_+}, \quad q_2 = \frac{1}{v_+^2}. \tag{145}$$

This path has the correct slope at the saddle point, except when $t = 1$. We have (again we assume in this notation that $a > 0$)

$$Y(-a,x) = \frac{j(a,x)}{\sqrt{w_+}} \int_{-u_+}^{\infty} e^{a\psi(q)} \left(\frac{dp}{dq} + i\right) \frac{dp}{\sqrt{1+\zeta}}, \tag{146}$$

where now

$$\psi(q) = \frac{1}{2}(p+iq)^2 - [\ln(1+\zeta) - \zeta]. \tag{147}$$

Again, the computation of $\Im\psi(q)$ needs some care for small values of q. This time we have

$$\Im\psi(q) = pq + \frac{\kappa\tau}{1+\kappa} - [\arctan\eta - \eta], \tag{148}$$

and

$$pq + \frac{\kappa\tau}{1+\kappa} = \frac{q^3}{v_+^2(1+\kappa)}\left[1 + u_+^2 + \frac{1+u_+ + u_+^2}{v_+}q + \frac{u_+ q^2}{v_+^2}\right]. \tag{149}$$

9.3 Monotonic region: $a < 0$, $t \geq 1$

The saddle points are now purely imaginary:

$$w_- = it - i\sqrt{t^2-1}, \quad w_+ = it + i\sqrt{t^2-1}. \tag{150}$$

The path of steepest descent starts at $w = 0$, runs through w_- and w_+ on the positive imaginary axis, and from w_+ to $+\infty$.

We consider the expressions (3.40) and (3.46) of [6] (but, as before, we consider $a < 0$ in our notation)

$$\begin{aligned} &U(a,x) + i\Gamma\left(\tfrac{1}{2} - a\right)V(a,x) = \\ &\sqrt{\frac{2}{\pi}}|a|^{1/4}\left[\frac{e^{\frac{1}{4}\pi i}}{F(a,x)}\int_0^{\frac{1}{2}\pi} e^{a\psi(\theta)}g(\theta)\,d\theta + i\frac{F(a,x)}{f(a)^2}\int_0^{r_+} e^{-a\widetilde{\phi}(v)}\frac{dv}{\sqrt{v}}\right], \end{aligned} \tag{151}$$

where $f(a)$ is as in Eq. (12).

$$\begin{aligned} &U'(a,x) + i\Gamma\left(\tfrac{1}{2} - a\right)V'(a,x) = \\ &\sqrt{\frac{2}{\pi}}|a|^{3/4}\left[\frac{e^{\frac{1}{4}\pi i}}{F(a,x)}\int_0^{\frac{1}{2}\pi} e^{-a\psi(\theta)}h(\theta)\,d\theta + i\frac{F(a,x)}{f(a)^2}\int_0^{r_+} e^{a\widetilde{\phi}(v)}(t-v)\frac{dv}{\sqrt{v}}\right], \end{aligned} \tag{152}$$

where ξ is given in Eq. (10),

$$\psi(\theta) = \tfrac{1}{2}r^2\cos 2\theta + 2tr\sin\theta - \ln r - t^2 - \tfrac{1}{2}, \tag{153}$$

$$h(\theta) = (t + iw)g(\theta), \tag{154}$$

$$g(\theta) = -\frac{e^{i\theta/2}}{\sqrt{r}}\left(\frac{dr}{d\theta} + ir\right) \tag{155}$$

and

$$\widetilde{\phi}(v) = \tfrac{1}{2}v^2 - 2tv + \ln v - \tfrac{1}{2}r_-^2 + 2tr_- - \ln r_-, \quad r_\pm = t \pm \sqrt{t^2-1}. \tag{156}$$

If we write

$$e^{\frac{1}{4}\pi i}g(\theta) = g_1(\theta) + ig_2(\theta),$$
$$e^{\frac{1}{4}\pi i}h(\theta) = h_1(\theta) + ih_2(\theta), \tag{157}$$

where $g_i(\theta)$ and $h_i(\theta)$, $i = 1, 2$, are real, we find that the scaled functions can be written:

$$\widetilde{U}(a,x) = \sqrt{\tfrac{2}{\pi}}|a|^{1/4}\, G_1, \tag{158}$$

$$\widetilde{U'}(a,x) = \sqrt{\frac{2}{\pi}}|a|^{3/4} H_1, \tag{159}$$

$$\widetilde{V}(a,x) = \frac{1}{\pi}|a|^{1/4}\left(\beta(|a|)G_3 + N(a,x)G_2\right), \tag{160}$$

$$\widetilde{V'}(a,x) = \frac{1}{\pi}|a|^{3/4}\left(\beta(|a|)H_3 + N(a,x)H_2\right), \tag{161}$$

where

$$N(a,x) = \frac{\sqrt{2\pi}}{\Gamma(\frac{1}{2}-a)F(a,x)^2}\,. \tag{162}$$

$\beta(|a|)$ is given by Eq. (21),

$$G_j = \int_0^{\frac{1}{2}\pi} e^{a\psi(\theta)} g_j(\theta)\, d\theta\,,\ \text{for } j = 1, 2\,, \tag{163}$$

$$G_3 = \int_0^{r_+} e^{-a\widetilde{\phi}(v)}\,\frac{dv}{\sqrt{v}}, \tag{164}$$

$$H_j = \int_0^{\frac{1}{2}\pi} e^{a\psi(\theta)} h_j(\theta)\, d\theta\,, \text{for } j = 1, 2\,, \tag{165}$$

and

$$H_3 = \int_0^{r_+} e^{-a\widetilde{\phi}(v)}(t-v)\frac{dv}{\sqrt{v}}. \tag{166}$$

The second term for the V-function and the derivative is always noticeable close to the turning points, that is close to $x^2/4 + a = 0$, because if $t = 1$ then $N(a,x) = \beta(|a|)$. For larger t, $N(a,x)$ may become very small; in particular, for $a = 0$ we have that $N(a,x) = \sqrt{2}e^{-x^2/2}$ which becomes negligible for large x. In these circumstances, the second term should be neglected in order to avoid underflow problems. Writing

$$N(a,x) = \beta(|a|)e^{4a\xi} \tag{167}$$

it is easy to avoid underflow problems by controlling the size of the argument in the exponential.

In the algorithm [5], the $\theta-$integrals in (151) and (152) are replaced by integrals along the half-line $\Im w = \Im w_+, \Re w \geq 0$. The slope at the saddle point w_+ is correct, except when $t = 1$. Taking real and imaginary parts and considering the integrals for the derivatives, this results in the computation of four integrals.

The $v-$integrals in (151) and (152) are split up into integrals over the intervals $[0, v_-]$ and $[v_-, v_+]$. So, together with the corresponding integrals for the derivatives, we again have to compute four integrals for the $V-$integrals.

We exploit common properties of these integrals and we compute the eight integrals in one algorithm, using the following Wronskian relation to verify if the numerical precision has been obtained:

$$G_1 H_3 - H_1 G_3 + \frac{N(a,x)}{\beta(|a|)}(G_1 H_2 - G_2 H_1) = \frac{\pi}{|a|\beta(|a|)}\,. \tag{168}$$

Let (see (150)) $w_\pm = iv_\pm$, $v_\pm = t \pm \sqrt{t^2-1}$. The $\theta-$integral in (151) equals

$$G = \int_0^\infty e^{a\psi(u)} \frac{du}{\sqrt{u + iv_+}}, \tag{169}$$

where

$$\psi(u) = \tfrac{1}{2}u^2 - \tfrac{1}{2}\ln\left(1 + u^2 v_-^2\right) + i\left[\arctan uv_- - uv_-\right]. \tag{170}$$

We scale by writing $u = \sigma p, \sigma = \sqrt{2/|a|}$, and obtain, using $v_- v_+ = 1$,

$$G = \frac{\sigma e^{-\frac{1}{4}\pi i}}{\sqrt{v_+}} \int_0^\infty e^{-\psi_r(p) - i\psi_i(p)} \frac{dp}{\sqrt{1 - iuv_-}}, \tag{171}$$

where

$$\psi_r(p) = (pv_-)^2\left[2v_+\sqrt{t^2-1} - \frac{1}{a}(pv_-)^2 A(\xi)\right], \tag{172}$$

$$A(\xi) = -\frac{\ln(1+\xi) - \xi}{\frac{1}{2}\xi^2}, \quad \xi = (uv_-)^2, \tag{173}$$

$$\psi_i(p) = -a\left[\arctan uv_- - uv_-\right]. \tag{174}$$

We replace the $p-$interval $[0, \infty)$ by $[0, p_0]$, substitute $p = rp_0$, and finally $r = \frac{1}{2}\mathrm{erfc}(-\rho)$, where $\mathrm{erfc}\, z = 1 - \mathrm{erf}\, z$ is the complementary error function. This gives

$$G \simeq \frac{\sigma e^{-\frac{1}{4}\pi i}}{\sqrt{\pi v_+}} \int_{-\infty}^\infty e^{-\rho^2 - \psi_r(p) - i\psi_i(p)} \frac{d\rho}{\sqrt{1 - iuv_-}}. \tag{175}$$

The value of p_0 is obtained by solving for p the equation

$$e^{-2v_+\sqrt{t^2-1}(pv_-)^2 - \frac{1}{a}(pv_-)^4} = \varepsilon/10. \tag{176}$$

This value is too small, but one Newton iteration using $\psi_r(p)$ gives a value that is too large, but which is accepted.

For the corresponding $\theta-$integral for the derivatives in (151), we have

$$H \simeq \frac{\sqrt{a}\sigma e^{-\frac{1}{4}\pi i}}{\sqrt{\pi v_+}} \int_{-\infty}^\infty e^{-\rho^2 - \psi_r(p) - i\psi_i(p)} \left(-\sqrt{t^2-1} + iu\right) \frac{d\rho}{\sqrt{1 - iuv_-}}. \tag{177}$$

In the representations of $\psi_r(p)$ and $\psi_i(p)$ we can control the precision by using special algorithms for $\ln(1+x)-x$ and $\arctan x - x$ for small x. Small values of u, p and r correspond with large negative values of ρ, where small values of the $\rho-$integrals happen, because of the factor $e^{-\rho^2}$. Hence, very accurate values of $\psi_r(p)$ and $\psi_i(p)$ are not needed for small values of p.

Next we have to consider (see (163))

$$G_{31} = \int_{v_-}^{v_+} e^{-a\widetilde{\phi}(v)} \frac{dv}{\sqrt{v}}, \tag{178}$$

where $\widetilde{\phi}(v)$ is given in (156) with $r_- = v_-$. Put $v = \sigma q + v_-$ to obtain

$$G_{31} = \sigma \int_0^{q_1} e^{-\psi(q)} \frac{dq}{\sqrt{\sigma q + v_-}}, \quad q_1 = \frac{v_+ - v_-}{\sigma} = \frac{2\sqrt{t^2-1}}{\sigma}, \tag{179}$$

where

$$\psi(q) = -a\left\{v_-\sqrt{t^2-1}p^2 - \left[\ln(1+p) - p + \tfrac{1}{2}p^2\right]\right\}, \quad p = \sigma v_+ q. \tag{180}$$

For large t we have

$$av_-\sqrt{t^2-1}p^2 \sim 4at^2\sigma^2, \tag{181}$$

and we take

$$\sigma = \frac{1}{2t\sqrt{|a|}} = \frac{1}{x}. \tag{182}$$

The next steps are: $q = q_1 r, r = \frac{1}{2}\mathrm{erfc}(-\rho)$. This gives

$$G_{31} = \frac{q_1\sigma}{\sqrt{\pi}} \int_{-\infty}^{\infty} e^{-\rho^2-\psi(q)} \frac{d\rho}{\sqrt{\sigma q + v_-}}. \tag{183}$$

For the integral

$$G_{32} = \int_0^{v_-} e^{-a\widetilde{\phi}(v)} \frac{dv}{\sqrt{v}}, \tag{184}$$

we put $v = v_- - \sigma q$, again with $\sigma = 1/x$. For the integral H_3 of (165) we proceed in the same manner.

10. COMPUTATIONAL ASPECTS.

In this last section, we provide some additional details on the numerical implementation of the different approximations given in this article.

10.1 Attainable accuracy: condition numbers.

The first important aspect to be considered is the impossibility of building an algorithm, based on fixed precision arithmetic, with uniform relative accuracy for any range of the parameters of the parabolic cylinder functions. The attainable relative accuracy is limited by the condition numbers of the functions with respect to their parameters. We can estimate the condition numbers by taking into account that the asymptotic behaviour of PCF is governed by the factor $f(a,x)$ (7).

Let us first study the condition numbers for $F(a,x) = |f(a,x)|$ and leave for later the condition numbers caused by the phase of $f(a,x)$. With this approximation, the condition number for the V-function with respect to a with fixed $t = x/(2\sqrt{a})$ can be estimated as follows

$$C_a(V) \equiv a\frac{\partial V(a,x)/\partial a}{V(a,x)} \sim C_a(F) \equiv a\frac{\partial F/\partial a}{F} = \log(e^{a/2}F)\,. \qquad (185)$$

This means that for large $|a|$ a relative error in a, $\epsilon_r(a)$, is amplified by a factor $|C_a| \sim \frac{|a|}{2}\log(|a|)$ when computing the V function. The same is true for the derivative and the U function and its derivative. Then, for instance, with a typical double precision machine-epsilon of $\epsilon = 2.2\,10^{-16}$, the best attainable relative accuracy when $|a| = 100$ is $\epsilon|C_a| \sim 10^{-13}$.

The condition number with respect to x and a fixed reads

$$C_x(V) \equiv x\frac{\partial V(a,x)/\partial x}{V(a,x)} \sim C_x(F) \equiv x\frac{\partial F/\partial x}{F} = x\sqrt{\frac{x^2}{4} + a}\,, \qquad (186)$$

which is the same as the condition with respect to t.

The next figure shows the regions determined by the conditions that both $|C_x(F)|$ and $|C_a(F)|$ are smaller than a given number (100 and 500).

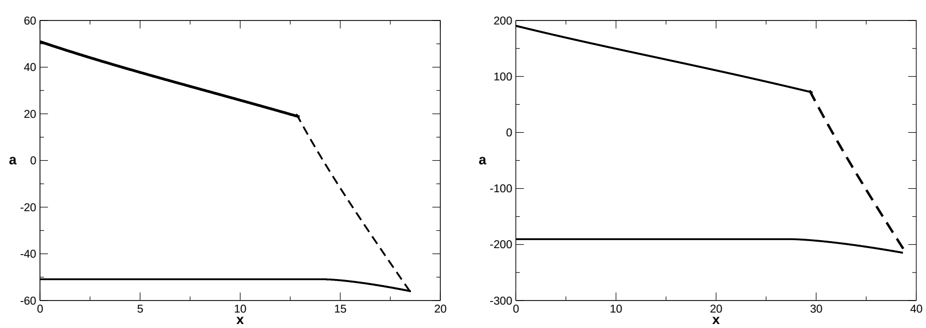

Figure 2. Regions where both condition numbers, $|C_x(F)|$ and $|C_a(F)|$ are smaller than 100 (left) and 500 (right). The dashed lines correspond to the condition with varying x and fixed a while the solid lines correspond to the condition for varying $|a|$ and fixed t.

The problem of bad conditioning can be circumvented by considering variable precision arithmetic with an increasing number of significant digits when the condition numbers become large. With fixed precision arithmetic, the best solution consists in scaling out the dominant exponential factor. This is also convenient for variable precision because the bad conditioning is isolated in the computation of an elementary function.

For scaled functions, the condition of the exponential of imaginary argument (oscillatory region) is the main concern. This is related to the evaluation of trigonometric functions for large arguments, which limits on the attainable accuracy, particularly in the oscillatory region. Considering the representation in Eqs. (55) and (130)-(133) we get that, for instance, the condition number for $\widetilde{V}$ with respect to

a for fixed t can be estimated to be

$$C_a(\tilde{V}) = a\frac{\partial\widetilde{V}/\partial a}{\widetilde{V}} \sim a\frac{\partial \sin\psi_1/\partial a}{\sin\psi_1} = 2|a|\eta/\tan\psi_1\,. \tag{187}$$

The condition number may get large for two reasons: first, because for large $|a|$ the argument of the trigonometric functions becomes large (factor $|a|$ in Eq. (187)); second because the function has zeros and at the zeros relative accuracy loses meaning (factor $\tan\psi_1$). The first effect becomes noticeable for large $|a|$ while the second one takes place also for small a. Notice that for $x=0$ the zeros are $U(-2k+1/2,0) = V'(-2k+1/2,0) = 0$, $V(-2k+3/2,0) = U'(-2k+3/2,0) = 0$, $k \in \mathbb{N}$ (Eq. (2)). This loss of precision is unavoidable with fixed precision arithmetic.

The moduli functions defined in Eq. (53) are not affected by the loss of precision caused by trigonometric function evaluations. In this sense, the routines in [7] can be considered satisfactory because they provide accurate values for $\widetilde{V}$ and $\widetilde{U}$ for moderate values of the parameters (not very close to zeros of the functions) and the moduli functions can be computed with uniform accuracy from the $\widetilde{V}$, $\widetilde{V'}$, $\widetilde{U}$ and $\widetilde{U'}$ values.

For positive a, the scaled V functions may also show large condition numbers when x is small. In particular, using Eq. (17) we see that, when $x=0$

$$C_a(\widetilde{V}) \sim \pi a\frac{\cos\pi a}{1+\sin\pi a} = \pi a/\tan\pi(a/2-3/4)\,. \tag{188}$$

This loss of precision is higher as larger a is considered and as values closer to the zeros of V (or V') are considered. The loss of precision due to these zeros is only noticeable in a very restricted region close to $x=0$. Considering Eqs.(34), we see that the loss of precision by cancellation will take place for $x << \sqrt{a}$, when the two terms are of similar size (see Eqs. (37) and (38)). As commented before, for very small t it is preferable to use Maclaurin series instead of uniform asymptotic expansions or integrals because the cancellations are explicit at $x=0$ with series (Eq. (17)).

It is important to stress that the Wronskian relations are insensitive to error degradation caused by the bad condition of the exponential and trigonometric functions. These errors are exactly canceled out in the Wronskian.

10.2 Applicability of the different methods

As commented before, when building an algorithm which is able to produce results which are well-conditioned, it is important to consider methods for which the dominant exponential factor can be factored out. This is also important in order to enlarge the range of computation of the functions. Among the different methods of computation considered, in all the asymptotic expansions, except the Poincaré-type expansion, the scaling factor $F(a,x)$ can be factored out exactly. The same is true for the integral representations considered. For both the Poincaré-type asymptotic expansion and Maclaurin series, the scaling factor $F(a,x)$ can not be factored out exactly and an exponential term remains. In both cases, the remaining factor does not overflow or underflow in the natural region of application of each of these methods ($x\sqrt{|a|}$ small for series and $x >> \sqrt{|a|}$ for Poincaré asymptotics).

The regions in the (x,a)-plane where the different methods can be applied are very similar for the U and V functions, except for Maclaurin series and the recurrence relations. The integral representations can be used almost without restrictions, except when $|a|$ is small, as can be understood by noticing that the Wronskian-type relations satisfied by the integrals are singular at $a=0$; additionally, the paths of integration and the saddle points become singular as $a\to 0$ for fixed x (because $t=x/(2\sqrt{|a|}\to\infty)$. Uniform asymptotic expansions in terms of elementary functions when $x^2/4+a>0$ have the double asymptotic property of being valid for fixed t and large a and for fixed $|a|$ and large t. This means that these expansions can also be used for quite small $|a|$ when x is large. Uniform asymptotic expansions in terms of Airy functions can be used in large regions of negative a and they are particularly useful around the curve of turning points $x^2/4+a=0$.

Maclaurin series are (as happens with recurrence relations) a method of computation for which the regions of application for U and V are quite different. Notice that both U and V are built from the combination of the same two series y_1 and y_2 (Eq. (14) but that U decreases exponentially as a becomes large for fixed $x>0$ and when $x>>a$ while V increases exponentially. Therefore, for large a and/or large x cancellations are expected in the computation of U.

Recurrence relations are the only method considered for which it is not possible to factor out satisfactorily the scaling factor. For this reason, they can only be applied for plain PCFs (not scaled). The application of recurrences starting from precalculated function values can be considered with the following restrictions: first, a method to compute accurately the starting values should be available; second (and related) the parameters should not be too large in order to avoid a bad conditioning for the computation of the starting values (also overflow/underflow problems, which are a less limiting condition); third, the recurrences should be applied in the stable direction for the solution under consideration.

The last condition implies that, when $x^2/4+a>0$, the $V(a,x)$ function should be computed in the direction of increasing a while the $U(a,x)$ has to be computed in the direction of decreasing a. For $x^2/4+a<0$ there is no preferred direction for the application of the recurrence and both directions are possible for both functions, but recurrence in this region has the problem of the bad condition of the function values (particularly near the zeros of the functions). In addition, using the recurrences when there is a preferred direction of application is a more stable process (when the right direction is chosen) than applying the recurrence when all the directions have the same condition.

For the U, we can consider starting values for positive a and then apply backward recurrence; the starting values can be, for instance, computed by means of the uniform asymptotic expansions of Eqs (28), (34). The starting a values should be large enough so that the asymptotic expansion is accurate enough but not too large in order to avoid bad conditioning. For the V the direction of application of the recurrence is the opposite and, if asymptotic expansions for computing the starting values are to be used, one should consider negative values of a of large enough modulus, but again not too large in order to avoid bad conditioning.

In the accompanying paper [7], we provide a detailed description of the selection of the regions in the (x,a)-plane where each method can be applied in order to compute the scaled functions for an aimed relative accuracy of $5\,10^{-14}$ (except close to the zeros of the functions).

ACKNOWLEDGMENTS

A. Gil acknowledges financial support from Ministerio de Ciencia y Tecnología (programa Ramón y Cajal). J. Segura acknowledges financial support from project BFM2003-06335-C03-02. N.M. Temme acknowledges financial support from Ministerio de Ciencia y Tecnología from project SAB2003-0113. The authors acknowledge financial support from project MTM2004-01367.

REFERENCES

[1] Abramowitz M., I. Stegun (Eds). *Handbook of Mathematical Functions.* National Bureau of Standards. Applied Mathematics Series, no. 55. U.S. Government Printing Office, Washington DC (1964).

[2] B. Fabijonas, D. Lozier, F.W.J. Olver. Computation of Complex Airy Functions and their Zeros using Asymptotics and the Differential Equation. ACM Trans.Math. Softw. 30 (2004) 471–490.

[3] B. Fabijonas. Algorithm 838: Airy Functions. ACM Trans.Math. Softw. 30 (2004) 491–501.

[4] L.W. Fullerton. Portable special function routines. Lecture Notes in Computer Science 57 (1977) 452–483. W. R. Cowell (Ed.), Portability of numerical software (Oak Brook, Illinois, 1976), Berlin: Springer-Verlag.

[5] A. Gil, J. Segura, N.M. Temme. Algorithm 819: AIZ, BIZ: Two Fortran 77 routines for the computation of complex Airy functions. ACM Trans.Math. Softw. 28 (2002) 325–336.

[6] A. Gil, J. Segura, N.M. Temme. Integral representations for computing real parabolic cylinder functions. Numer. Math. 98 (2004) 105–134.

[7] A. Gil, J. Segura, N.M. Temme. Algorithm XXX. Real Parabolic Cylinder Functions $U(a,x)$, $V(a,x)$ (in this same issue).

[8] J. C. P. Miller. On the choice of standard solutions for a homogeneous linear differential equation of the second order. Quart. J. Mech. Appl. Math.3 (1950) 225–235.

[9] H. Takahashi, M. Mori. Quadrature formulas obtained by variable transformation. Numer. Math. 21 (1973) 206–219.

[10] F.W.J. Olver. Uniform asymptotic expansions for Weber parabolic cylinder functions of large orders. J. Res. Nat. Bur. Standards Sect. B, 63B (1959) 131–169.

[11] J. Segura, A. Gil. Parabolic Cylinder Functions of integer and half-integer orders for nonnegative arguments. Comput. Phys. Commun. 115 (1998) 69–86.

[12] N.M. Temme. Numerical and asymptotic aspects of parabolic cylinder functions. J. Comp. Appl. Math., 121 (2000) 221–246.